ACS Biomaterials SCIENCE & ENGINEERING

Article

pubs.acs.org/journal/abseba

Synthesis of Heparin-Immobilized, Magnetically Addressable Cellulose Nanofibers for Biomedical Applications

Lijuan Hou,[†,‡,∥] W. M. Ranodhi N. Udangawa,[†,§,∥] Anirudh Pochiraju,[□] Wenjun Dong,[‡,△] Yingying Zheng,[‡] Robert J. Linhardt,[§,⊥,∥,○] and Trevor J. Simmons*[,#,○]

[‡]Center for Nanoscience and Nanotechnology, Zhejiang Sci-Tech University, 5 Second Avenue, Xiasha Higher Education Zone, Hangzhou 310018, PR China

[§]Department of Chemistry and Chemical Biology, [⊥]Chemical and Biological Engineering, [∥]Center for Biotechnology and Interdisciplinary Studies, [#]The Center for Future Energy Systems, [□]Department of Biological Sciences, and [○]Rensselaer Nanotechnology Center, Rensselaer Polytechnic Institute, 110 Eighth Street, Troy, New York 12180, United States

[△]School of Materials Science and Engineering, University of Science and Technology Beijing, 30 Xueyuan Road, Haidian District, Beijing 100083, PR China

Supporting Information

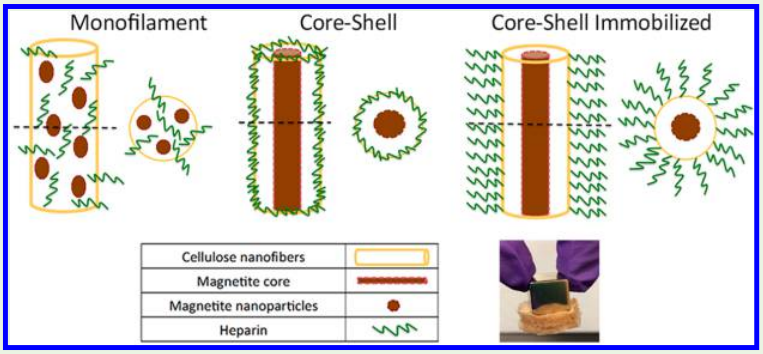

ABSTRACT: Magnetically responsive heparin-immobilized cellulose nanofiber composites were synthesized by wet-wet electrospinning from a nonvolatile, room-temperature ionic liquid (RTIL), 1-methyl-3-methylimidazolium acetate ([EMIM]-[Ac]), into an aqueous coagulation bath. Superparamagnetic magnetite (Fe_3O_4) nanoparticles were incorporated into the fibers to enable the manipulation of both dry and wet nanofiber membranes with an external magnetic field. Three synthetic routes were developed to prepare three distinct types of nanocomposite fibers: cellulose-Fe_3O_4–heparin monofilament fibers, cellulose-Fe_3O_4–heparin core–shell fibers with heparin covalently immobilized on the fiber surface, and cellulose -Fe_3O_4 core–shell fibers with heparin physically immobilized on the fiber surface. These nanocomposite fibers were characterized by electron microscopy to confirm their coaxial structure and the fiber dimensions (fiber diameter 0.2–2.0 μm with 0.1–1.1 μm core diameter). Thermogravimetric analysis, liquid chromatography–mass spectrometry, Fourier transform infrared and X-ray diffraction spectroscopy provided detailed compositional analysis for these nanocomposite fibers, confirming the presence of each component and the surface accessibility of the heparin. The anticoagulant activity of immobilized heparin on the nanocomposite fiber surfaces was evaluated and confirmed by antifactor Xa and antifactor IIa assays.

KEYWORDS: *cellulose, magnetite, heparin, electrospinning, core–shell, nanofiber*

INTRODUCTION

Innovative nanomaterials functionalized with heparin have advanced significantly in recent years in part due to the remarkable growth in nanobiotechnology.[1−7] Heparin is a biocompatible, biodegradable, water-soluble natural polysaccharide, which has been used as an anticoagulant drug for nearly a century. This negatively charged glycosaminoglycan is widely used as an injectable anticoagulant and to make anticoagulant surfaces in biomedical devices.[8−10] When a foreign material contacts a human tissue, such as circulating blood, an aggressive response occurs resulting in the activation of the coagulation cascade and platelets leading to clot formation. This complex process of thrombus formation involves the participation of a number of cell types, tissue factors, enzymes, and their cofactors. Thrombus formation may cause a malfunction of an implanted device with the outcome adversely impacting a patient's health. Heparin is used to reduce the thrombogenicity of blood contacting devices by

Received: May 18, 2016
Accepted: August 17, 2016
Published: August 17, 2016

DOI: 10.1021/acsbiomaterials.6b00273
ACS Biomater. Sci. Eng. 2016, 2, 1905−1913

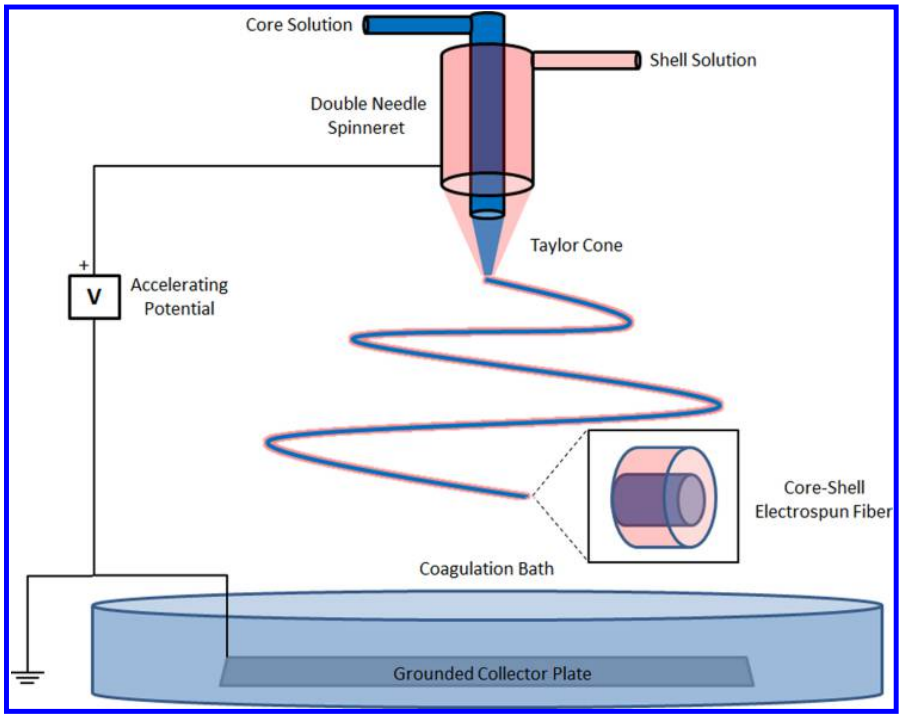

Figure 1. Electrospinning of core−shell fibers is accomplished using a coaxial spinneret. Two different solutions are pumped at different rates into the spinneret and accelerated by a potential, forming a Taylor cone and elongating into fibers that are collected in a grounded coagulation bath.

immobilizing it on a polymer surface and grafting it onto the blood-contacting surface of biomedical devices.[10] Heparin also interacts with a variety of proteins that have heparin-binding peptide domains.[11] These interactions enable heparin to be used in conjugation with biomolecules for numerous biomedical applications including the controlled release of biological factors in cells and throughout the human body.[12]

Several types of nanocomposite materials have been fabricated by functionalizing nanomaterials and polymers with heparin.[9] In most cases, these nanomaterials were used as a solid support or to impart novel properties. Such composite materials have been used in medical devices ranging from extracorporeal blood filters[7] to venous catheters.[10,13−15]

Magnetic nanoparticles (NPs) are of interest in the field of biomedicine.[16] The magnetic properties of these NPs depend on their size. In contrast to bulk Fe_3O_4, which is a multidomain ferromagnetic material that exhibits permanent magnetization in the absence of an external magnetic field, Fe_3O_4 NPs < 20 nm in size contain a single magnetic domain and exhibit superparamagnetism.[17] Each of these small Fe_3O_4 NPs contain a single paramagnetic magnetic domain that flips randomly at body temperature and aligns their magnetic moment in the presence of an external magnetic field. Consequently, superparamagnetic NPs are ideal for biomolecular detection, imaging and drug delivery applications due to their negligible agglomeration at body temperature. These NPs can also be functionalized with surfactant layers to avoid the risk of agglomeration and thereby achieve greater stability over longer periods of time.

In biomedical applications, the most commonly utilized forms of superparamagnetic iron oxide magnetic NPs, also referred to as SPIONs, are maghemite (γ-Fe_2O_3) and magnetite (Fe_3O_4).[17,18] SPIONs are generally well-tolerated in biological systems and are similar in size to biomacromolecules. Therefore, they are ideal substrates to be functionalized with biomolecules to produce nanobioconjugates for biomedical applications.

Cellulose is the most abundant biopolymer on earth. It is primarily found in the cell walls of plants, which account for the majority of terrestrial biomass. Therefore, cellulose is renewable and biocompatible, and possesses excellent thermal and mechanical properties. Cellulose can be used to make fibers with high tensile strength because of its highly crystalline linear structure.[19] Cellulose nanofibers have become quite popular among research scientists, particularly in the field of biomedicine.[19−23]

Electrospinning is a fiber fabrication technique that is widely used in the production of micron and nanometer scale fibrous materials. Electrospinning can be divided in to two major categories depending on the method of fiber collection. Wet−dry electrospinning was the first method to be developed and involves dissolution of the desired polymer in a volatile solvent that evaporates in the electrospinning process leaving dry polymer fibers on a collector plate.[24] Wet−wet electrospinning was then developed where a polymer is dissolved in a primary solvent and electrospun into a coagulation bath filled with a secondary cosolvent that is miscible with the primary solvent, but is a nonsolvent for the polymer.[25] The electrospun polymer fibers can then be dried either by desiccation or freeze-drying. Electrospinning can also be varied based on the type of spinneret used in the process. In contrast to single nozzle spinnerets, coaxial, and multiaxial spinnerets allow core−shell fibers to be produced (Figure 1). This technique will concentrate the nanomaterials either in the core or in the shell of the electrospun fiber.[26]

DOI: 10.1021/acsbiomaterials.6b00273
ACS Biomater. Sci. Eng. 2016, 2, 1905−1913

With the discovery of a class of solvents known as room temperature ionic liquids (RTILs), it became possible to electrospin a variety of polymers that are insoluble in conventional solvents.[27−32] Most polysaccharides are highly complex and challenging to dissolve, and accordingly cellulose is insoluble in both aqueous and organic solvents. Heparin is soluble in few volatile organic solvents but readily soluble in water. However, both polymers are soluble in several RTILs allowing them to be used in the preparation of stable composite materials.[33,34]

The approach being reported in the current study involves the synthesis of nanoscale fibers from biodegradable and biocompatible polymers that are functionalized with nanomaterials and biomacromolecules to obtain nanocomposite materials with tunable properties for biomedical applications. SPIONs are incorporated into a cellulose matrix that is modified with heparin to construct anticoagulant and magnetically addressable biocompatible nanocomposites. Heparin-coated cellulose nanofibers were synthesized by wet−wet electrospinning with Fe_3O_4 SPIONs incorporated to allow for the movement of the nanofibers produced through the application of an external magnetic field in both wet and dry states. Cellulose itself is biocompatible but not completely blood compatible,[35] therefore heparin was immobilized onto cellulose fibers to achieve improved blood compatibility and SPIONs were incorporated into the fibers to enable fiber manipulation in both the wet and dry state with the application of an external magnetic field. In this way, cellulose nanofibers that are well tolerated in biological systems have been made suitable for direct blood contact and can be externally manipulated through noninvasive application of a magnetic field.

MATERIALS AND METHODS

Materials. Cellulose pulp (degree of polymerization ca. 1100) was obtained from Weyerhaeuser Co. (Oglethorpe, GA, USA). The RTIL 1-ethyl-3-methylimidazolium acetate ([EMIM][Ac]) was obtained from Sigma-Aldrich (St. Louis, MO, USA). Lyophilized USP heparin sodium (from porcine intestinal mucosa) was obtained from Celsus Laboratories Inc. (Cincinnati, OH, USA). Magnetite (Fe_3O_4) NPs (superparamagnetic, ca. 5 nm in diameter, > 30 emu/g magnetization, 30 wt % oleic acid coating) were purchased from NN-Laboratories (Fayetteville, AK, USA). Reagent grade cyanogen bromide (97%) and sodium hydrogen carbonate (≥95%) were obtained from Sigma-Aldrich (St. Louis, MO, USA). Sodium hydroxide pellets (≥97.0%) were purchased from Fisher Scientific (Springfield, NJ, USA). Heparin disaccharide standards (see the Supporting Information) were purchased from Iduron (Manchester, UK). HPLC grade ammonium acetate, calcium chloride, acetic acid and acetonitrile were purchased from Fisher Scientific (Springfield, NJ, USA). Tributylamine was purchased from Sigma−Aldrich (St. Louis, MO, USA). BIOPHEN Heparin Anti-IIa (or Anti-Xa) kit was obtained from ANIARA Diagnostica (West Chester, OH, USA).

Recombinant *Flavobacterium heparinum* heparin lyase I, II, III (Enzyme Commission (EC) numbers 4.2.2.7, 4.2.2.X, 4.2.2.8)[36] were expressed in *Escherichia coli* with a His-tag. Expression and purification were carried out in house.

Electrospinning Solutions. Cellulose pulp was dissolved in [EMIM][Ac] by mechanical stirring at 80 °C for several hours to prepare a 1.5 wt % homogeneous cellulose solution. Cellulose−Fe_3O_4−heparin solutions (0.8, 0.17, 0.7 wt %, respectively) were prepared by first dissolving Fe_3O_4 NPs in [EMIM][Ac] and then adding cellulose pulp and sodium heparin in to the homogeneous NP solution. The final mixture was then further mechanically stirred at 80 °C overnight to form a homogeneous solution. The Fe_3O_4 NP core solution (2 wt %) was prepared by mechanically stirring Fe_3O_4 NPs in [EMIM][Ac] at 80 °C to form a homogeneous NP solution. Cellulose/heparin blended shell solution was prepared by dissolving cellulose (1.5 wt %) and (1 wt %) heparin in [EMIM][Ac].

Electrospinning Procedure. Electrospinning experiments were carried out at 20 ± 3 °C with relative humidity of 30 ± 5%. The 1.5 wt % cellulose solution was placed in a 10 mL Luer lock syringe and connected by PTFE tubing to the spinneret (MECC, Ogori, Fukuoka, Japan) PTFE. The high voltage supply (Spellman CZE1000R, Hauppauge, NY, USA) was maintained at approximately 18 kV DC. The distance between the needle tip and the surface of the water in the coagulation bath was fixed at 20 cm. A mechanical syringe pump (NE-1000, New Era Pump System Inc., Wantagh, NY, USA) was used to feed the electrospinning solution at a constant rate of 40 μL/min to obtain continuous fibers. Electrospun fibers were collected in the coagulation bath filled with distilled water coagulate and solidify the fibers by removing the [EMIM][Ac] (Figure 1). Finally, the fibers were washed several times with fresh water and subsequently freeze-dried to obtain the final cellulose nanofiber product.

The cellulose−Fe_3O_4−heparin solutions (0.8, 0.17, 0.7 wt %, respectively) were electrospun to produce cellulose−Fe_3O_4−heparin monofilament nanofibers with a similar procedure, but with an increased diameter (18 ga., I.D. 1.27 mm) of the aluminum needle connected to the spinneret.

Cellulose−Fe_3O_4 core−shell fibers were fabricated using a coaxial−electrospinning technique. The coaxial spinneret (MECC, Ogori, Fukuoka, Japan) was fitted with blunt tip aluminum needles (core, I.D. 1.27 mm; shell, I.D. 2.50 mm). The 1.5 wt % cellulose solution (shell) and 2 wt % Fe_3O_4 solution (core) were placed in two separate 10 mL syringes and connected independently to their respective ports on the spinneret using PTFE tubing. A potential of 15 kV was applied between the spinneret and the collector. High voltage was applied between the spinneret and the electrically grounded collector, which was a 7.5 × 7.5 cm sheet of aluminum foil on the bottom of the coagulation bath. The distance between the needle tip and the surface of the water in the coagulation bath was fixed at 20 cm. Two syringe pumps (NE-1000, New Era Pump System Inc., Wantagh, New York, USA) were used to feed the core and shell electrospinning solutions at constant rates of 30 μL/min and 100 μL/min, respectively, to obtain continuous core−shell nanofibers. Finally, the fibers were washed several times with water and then freeze-dried to obtain cellulose−Fe_3O_4 core−shell nanofibers.

Cellulose−Fe_3O_4 core−shell fibers with heparin blended into the shell were also fabricated by coelectrospinning. The diameter of the inner needle and outer spinneret needles were 0.94 mm and 2.50 mm, respectively. The distance between the spinneret tip and aluminum collector electrode was fixed at 15 cm. In order to obtain continuous electrospinning and optimal fiber production, total flow rate and applied voltage were optimized with typical values ranging from 200 to 230 μL/min and 12−16 kV respectively. Electrospun fibers were collected into a coagulation bath, which was filled with a water/ethanol mixture to remove IL, thereby solidifying the fibers. The fibers formed an entangled web (fiber mat) in the coagulation bath and were subsequently removed and washed with ethanol and freeze-dried under vacuum. Double-distilled deionized (DD-DI) water was used for all of the work being reported.

Covalent Immobilization of Heparin on Electrospun Cellulose-Fe_3O_4 Core−Shell Fibers. A two-step reaction scheme was used to covalently immobilize heparin to the surface electrospun cellulose nanofibers. The activation of polysaccharides such as cellulose with cyanogen bromide for the immobilization of heparin has been previously described.[37−40] A 2 mL aliquot of an aqueous cyanogen bromide solution (50 mg/mL) is treated with an aqueous 2 M NaOH solution until the solution pH 11. Cellulose-Fe_3O_4 core−shell fibers are added to the mixture while maintaining the pH at 11. After 15 min the fiber sample is washed with cold water on a fritted glass filter under suction until the filtrate produces a negative $AgNO_3$ test, confirming the absence of bromide. If not immediately used, the activated fibers could be stored at −20 °C for 24 h. The activated fibers are washed several times with cold water and a cold sodium bicarbonate solution (0.1 M) before reacting with a heparin solution

DOI: 10.1021/acsbiomaterials.6b00273
ACS Biomater. Sci. Eng. 2016, 2, 1905−1913

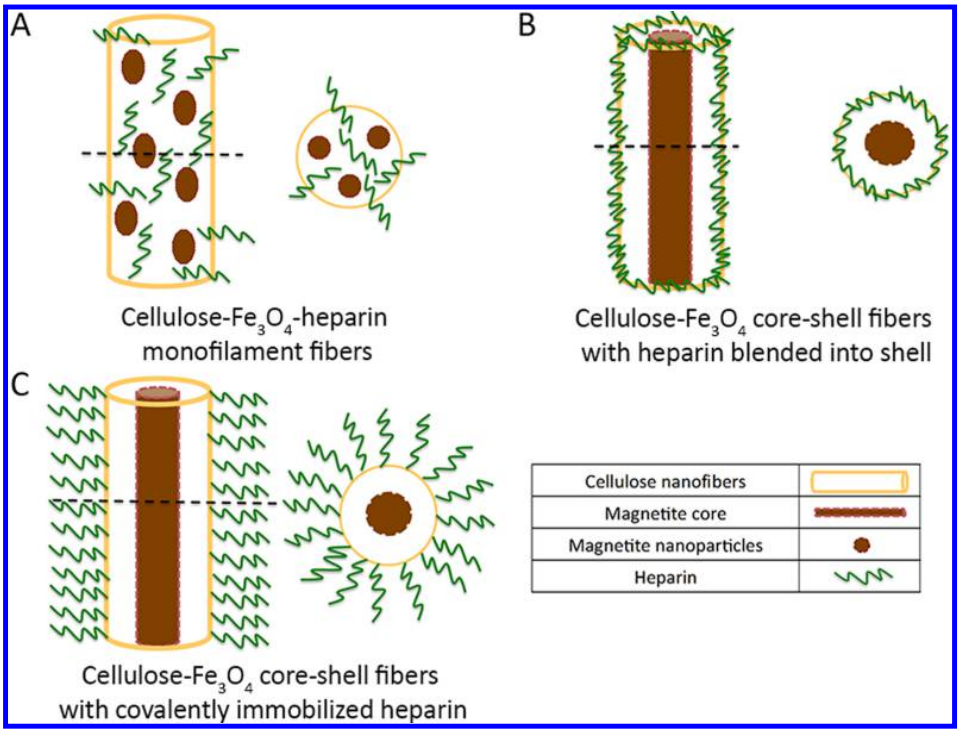

Figure 2. Structure of nanofibers. (A) Cellulose-Fe_3O_4-heparin monofilament fibers with entrapped Fe_3O_4 NPs and heparin. (B) Cellulose-Fe_3O_4 core−shell nanofiber with internal Fe_3O_4 NP core and cellulose shell blended with heparin. (C) Cellulose-Fe_3O_4 core−shell nanofiber with with internal Fe_3O_4 NP core and cellulose shell with covalently immobilized heparin.

(20 mg/mL in 0.1 M $NaHCO_3$). Finally, the covalently coupled cellulose−Fe_3O_4 core−shell fibers with covalently immobilized heparin were washed with cold distilled water under suction filtration for several minutes and then freeze-dried to obtain dried nanofibers.

Characterization. Attenuated total reflectance-Fourier transform infrared (ATR-FTIR) spectra of both activated fibers and heparin immobilized fibers were collected with a Varian 660-IR FTIR spectrophotometer (Varian Inc. USA) using the diffuse reflectance sampling accessory with a zinc selenide internal reflection element (IRE). FEI-VERSA field-emission scanning electron microscope (FEI, Hillsboro, OR, USA) was used to image the electrospun nanofiber samples at an accelerating voltage of 20.0 kV. The average fiber diameters were determined from SEM images of over 100 individual fibers, using the NIH ImageJ software. (National Institute of Health, MD, USA) JEOL-JSM-840 scanning electron microscope (SEM) was used to conduct energy dispersive X-ray spectroscopic (EDX) analysis of fiber samples. The EDX spectra were analyzed using INCA Microanalysis Suite software. The core−shell and monofilament fiber samples were further analyzed using transmission electron microscope (TEM). The samples were dispersed in ethanol and deposited on lacey carbon coated 200 mesh copper grids and imaged at an accelerating voltage of 200 kV using the JEOL-JEM-2011 TEM (JEOL Ltd., Tokyo, Japan). The average fiber diameters were determined from TEM images using ImageJ. Liquid chromatography (LC) -mass spectrometry (MS) (Agilent 6300 Ion Trap LC/MS Systems, CA 95051, USA) was used to verify the presence of heparin in both the core−shell fibers and monofilament fibers. Agilent poroshell 120, EC-C18 column (2.1 × 100 mm, 2.7 mm) of the Agilent 1200 LC system was employed to achieve the chromatographic separation at 55 °C. The separated disaccharides were then subjected to a full range mass spectrometric analysis (200−900 Da) in negative ionization mode with a skimmer voltage of −40.0 V, a capillary exit of −40.0 V and a source temperature of 350 °C. Liquid nitrogen was used as the drying and nebulizing gas at a flow rate of 8 L/min and a pressure of 40 psi, respectively. Thermogravimetric analysis (TGA) was performed using a computer-controlled TA Instruments TGA Q50 apparatus (New Castle, DE, USA) under a nitrogen/oxygen atmosphere. The samples were heated from room temperature to 600 °C at a constant heating rate of 20 °C/min. The fiber samples were then analyzed using a Bruker D8-DISCOVER X-ray diffractometer (XRD) with a $Cu_{K\alpha}$ radiation source and a pyrolytic graphite monochromator. Data analysis was performed using the Origin Pro software. (Northampton, MA, USA)

Anticoagulant Activity of Immobilized Heparin. Electrospun nanofiber samples were subjected to *in vitro* antifactor IIa and antifactor Xa activity assays using BIOPHEN Heparin anti-IIa (or Anti-Xa) kit (ANIARA Diagnostica, West Chester, OH). First, the fiber samples were washed thoroughly with DD-DI water under suction filtration for several minutes to remove all leachable heparin and other possible contaminants. Approximately 100 μg of each dry fiber sample and an aliquot of reaction buffer (positive control) were placed in a 96 well plate along with the reagent 1, 2, and 3 of the kit, which contains antithrombin III, factor IIa (or factor Xa) and their chromogenic substrates, respectively. All the samples and reagents were preincubated at 37 °C for 10 min. Then, the fiber samples were mixed with reagent 1 of the kit to start the assay at 37 °C. Next, reagents 2, 3, and 20% acetic acid were added respectivley at exactly 2, 4, and 5 min (or 6 min for anti-Xa) time points. The reaction mixtures were then filtered by 0.45 μm (or 0.22 μm) PVDF membrane (Millex-HV, Millipore, Cat. # SLHVR04NL). Finally, the absorbance of a 100 μL portion of the filtered reaction mixtures were measured at 405 nm. All of the fiber samples, the positive control and the blank were measured in triplicates. The final mean absorbance of the samples was obtained by subtracting the mean absorbance of the blank from each of the absorbance data.

RESULTS AND DISCUSSION

A variety of cellulose nanofibers were prepared by wet-wet electrospinning from RTIL. Some of these fibers were produced from a mixture of cellulose, Fe_3O_4 NPs, and heparin in RTIL to form cellulose-Fe_3O_4-heparin monofilament fibers

DOI: 10.1021/acsbiomaterials.6b00273
ACS Biomater. Sci. Eng. 2016, 2, 1905−1913

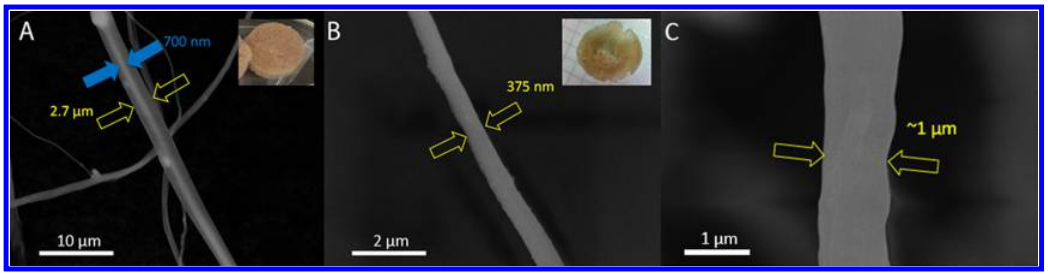

Figure 3. SEM imaging of nanofibers with photographs inset. (A) Cellulose−Fe_3O_4 core−shell nanofiber with internal Fe_3O_4 NP core and cellulose shell with covalently immobilized heparin. (B) Cellulose−Fe_3O_4−heparin monofilament fibers with entrapped Fe_3O_4 NPs and entrapped heparin. (C) Cellulose−Fe_3O_4 core−shell nanofiber with internal Fe_3O_4 NP core and cellulose shell blended with heparin.

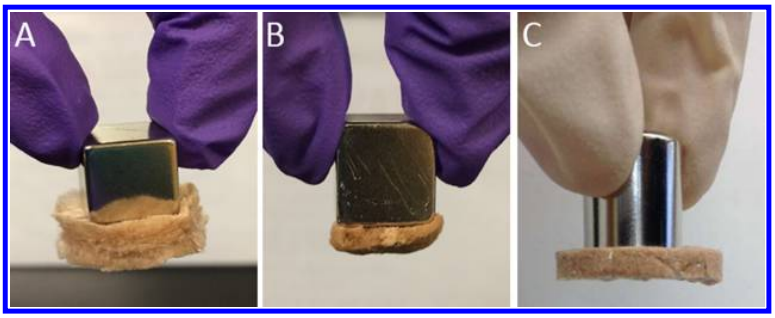

Figure 4. Demonstration of magnetic properties of dry cellulose fiber composites. (A) Cellulose−Fe_3O_4 coreshell nanofiber with internal Fe_3O_4 NP core and cellulose shell with covalently immobilized heparin. (B) Cellulose−Fe_3O_4−heparin monofilament fibers with entrapped Fe_3O_4 NP s and heparin. (C) Cellulose−Fe_3O_4 core−shell nanofiber with internal Fe_3O_4 NP core and cellulose shell with immobilized heparin.

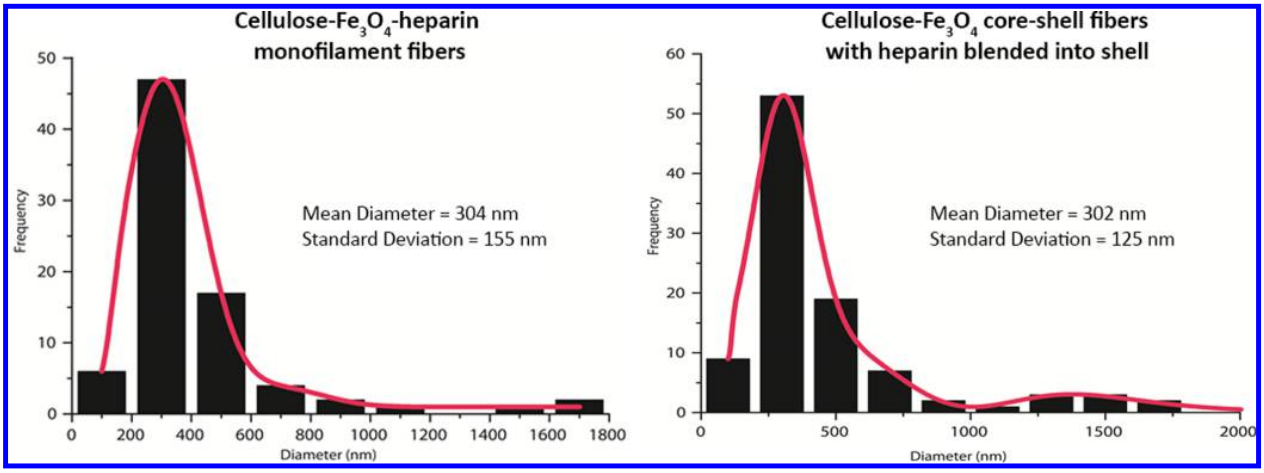

Figure 5. Histograms of fiber diameters observed during SEM imaging.

(Figure 2A). Others were spun coaxially with a magnetic Fe_3O_4 core and heparin surface coating that was either a blend of cellulose and heparin in the shell (Figure 2B) or with heparin covalently immobilized on the surface of the cellulose shell (Figure 2C).

Electrospinning from a mixed solution of cellulose−Fe_3O_4−heparin in RTIL resulted in monofilament fibers with Fe_3O_4 NPs distributed throughout the interior of the fibers (Figure 2B), with only a small minority of the Fe_3O_4 NPs on the fiber surface. When the fiber jet first enters the coagulation bath an intermediate fiber hydrogel is rapidly formed. Water flows in to replace the RTIL diffusing outward into the water forming the fiber hydrogel. This hydrogel is then washed with fresh water and freeze-dried. These fibers have a relatively small number of Fe_3O_4 NPs on their surface, migrating to the fiber surface during the hydrogel state of coagulation process (see the Supporting Information). During this migration process some NPs will remain physically trapped at the surface of the electrospun fibers. The smallest fibers observed from TEM showed a higher density of the Fe_3O_4 NPs on their surfaces, likely due to the shorter migration distance.

The purpose of Fe_3O_4 NPs in the nanocomposite fibers is to allow for the manipulation of the fibers in the presence of an applied external magnetic field. Although Fe_3O_4 is considered generally nontoxic to humans, it can cause cytotoxic effects when injected into the bloodstream. Therefore, to minimize potential complications, we encapsulated the Fe_3O_4 NPs within a cellulose shell by coaxial electrospinning.

DOI: 10.1021/acsbiomaterials.6b00273
ACS Biomater. Sci. Eng. 2016, 2, 1905−1913

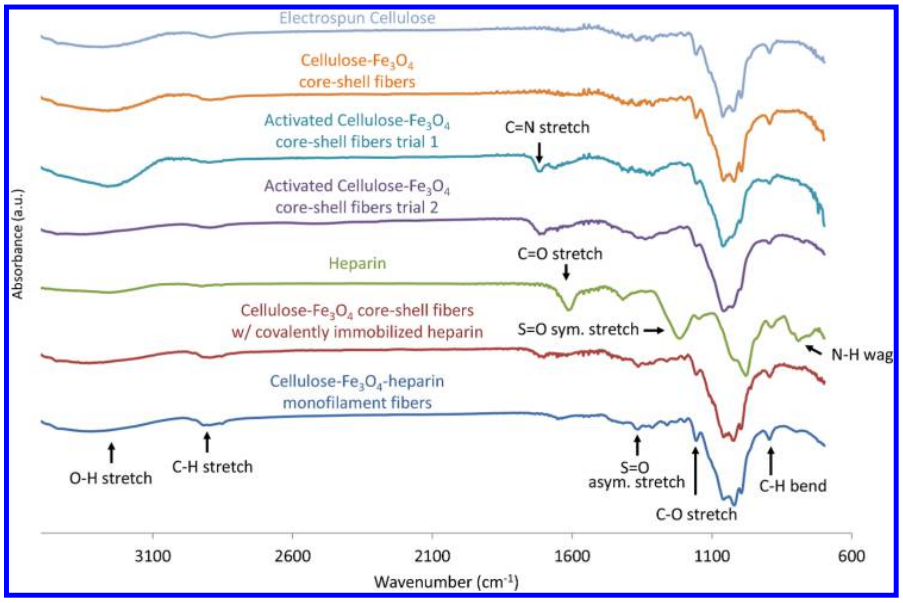

Figure 6. ATR FT-IR of nanofiber composites. The C═N peak at 1708 cm^{-1} confirms activation with cyanogen bromide, after covalent attachment of heparin the intensity of the O−H stretching peak and C═N stretching peak were significantly decreased. The spectra of cellulose-Fe_3O_4 core−shell nanofibers with covalently immobilized heparin show two small peaks at 1207 and 1411 cm^{-1} that correspond to S═O symmetric and asymmetric stretching vibrations, respectively. The IR spectrum of monofilament fibers showed four characteristic IR peaks of heparin including the two S═O stretching peaks and two other peaks at 1645 and 782 cm^{-1} that correspond to C═O stretching and N−H wagging vibrations of the amide group, respectively.

The magnetic properties of the monofilament and core−shell nanofibers were investigated empirically with a 15 g neodymium block magnet (NdFeB-Ni coating) with a surface field of approximately 6400 gauss. Both of the composite fiber mats displayed significant magnetic character in both dry (Figure 3) and wet states. When suspended in water, monofilament composite fibers showed more attraction to the Nd magnet than the core−shell fibers (see Videos S1 and S2). This could be due to the magnetite NPs present on the surface of the monofilament fibers or due to a slightly higher concentration of Fe_3O_4 NPs in the monofilament fibers resulting in more magnetically responsive fiber mats. Additionally, the cellulose-Fe_3O_4 core−shell nanofibers have isolated magnetite cores encapsulated within a cellulose shell, which may act as an insulating shield both between fibers and between the fiber mat and the Nd magnet, weakening the fiber response to applied external magnetic fields. An order of magnitude more Fe_3O_4 NPs was required in the synthesis of the cellulose-Fe_3O_4 core−shell nanofibers to achieve the same magnetic properties observed for the cellulose- Fe_3O_4-heparin monofilament fibers (2.0 wt % Fe_3O_4 in cellulose for core−shell fibers compared to 0.2 wt % Fe_3O_4 in cellulose for monofilament fibers).

Fiber morphology was next analyzed with electron microscopy, with average diameters of approximately 300 nm for all samples studied (see Figure 4). The imaging revealed a broad distribution of cellulose fibers, with a standard deviation of approximately 150 nm (see Figure 5). SEM images of larger core−shell fibers clearly exhibit a Fe_3O_4 NP core, with the imaging aided by the higher atomic number of Fe backscattering more electrons thereby providing an increased visible contrast. The Fe_3O_4 NPs core in smaller diameter fibers was observable only by TEM (see the Supporting Information).

Although simple monofilament fibers may be bioactive and biocompatible, prolonged use of these can materials in the body may leach heparin into body fluids. Free heparin in the bloodstream can cause morbidity and mortality in patients, with a potential for severe postoperative bleeding. Also Fe_3O_4 NPs on the surface could potentially dislodge and result in cytotoxicity. In order to overcome these possible complications, heparin was covalently immobilized onto electrospun cellulose−Fe_3O_4 core−shell fibers. A simple two-step reaction scheme was used to chemically couple heparin. This process involves the activation of the surface hydroxyl groups of the cellulose fiber and subsequently reacting the activated fiber surface with heparin. Even though cyanogen bromide activation is the most convenient method of activation, the mechanism of coupling with heparin is poorly understood.[40] ATR-FTIR spectra of cellulose nanofibers, cellulose−Fe_3O_4 core−shell nanofibers, activated cellulose−Fe_3O_4 core−shell nanofibers, cellulose−Fe_3O_4 core−shell nanofibers with heparin blended into the shell and cellulose−Fe_3O_4−heparin monofilament nanofibers showed the same cellulose characteristic IR peaks at 3305, 2885, 1153, and 893 cm^{-1}, corresponding to O−H, C−H, C−O stretching, and C−H bending vibrations, respectively (see Figure 6).[23] The cyanogen bromide activated fibers show a peak at 1708 cm^{-1} that corresponds to C═N stretching vibration confirming that activation has taken place. After the covalent immobilization of heparin to the activated fibers the intensity of the O−H stretching peak and C═N stretching peak were significantly decreased indicating the covalent attachment of heparin. The spectra of cellulose−Fe_3O_4 core−shell nanofibers with heparin blended into the shell showed two small characteristic IR peaks of heparin at around 1207 and 1411 cm^{-1} that correspond to S═O symmetric and asymmetric stretching vibrations, respectively. The IR spectrum of monofilament fibers showed four characteristic IR peaks of heparin including the two S═O stretching peaks and two new peaks at around 1645 and 782 cm^{-1} that correspond to C═O

DOI: 10.1021/acsbiomaterials.6b00273
ACS Biomater. Sci. Eng. 2016, 2, 1905−1913

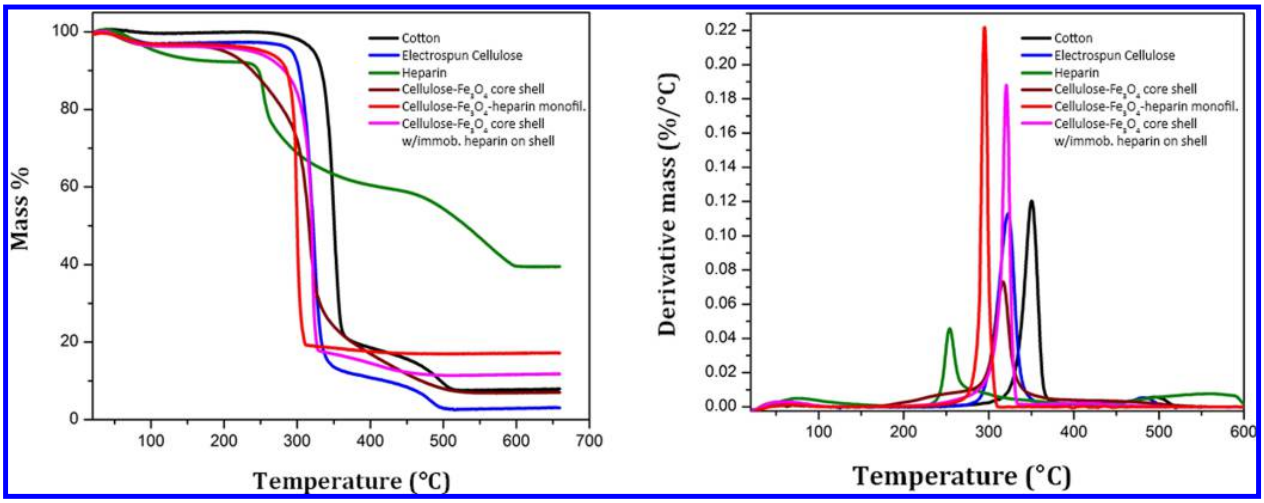

Figure 7. TGA analysis of nanofiber composites in dry air. Pure cellulose shows the lowest residual ash. Heparin shows a significant ash residue above 600 °C as expected, and similar residual ash is seen in the heparin containing samples. For all fibers studied, the heterogeneous monofilament fibers exhibited the lowest temperature onset of thermal degradation, and the natural cotton showed the highest thermal stability.

stretching and N−H wagging vibrations of the amide group, respectively.[2] Thus, the FTIR results confirm the presence of heparin in the nanofibers.

The EDX spectra of all of the heparin containing fibers showed characteristic peaks for S and N, confirming the presence of heparin in the fibers (see the Supporting Information). The EDX spectrum of cellulose showed characteristic peaks corresponding to carbon and oxygen at 0.277 and 0.525 keV, respectively. The EDX spectra of cellulose−Fe_3O_4−heparin monofilament fibers and the cellulose-Fe_3O_4 core−shell fibers with heparin blended into the shell exhibited characteristic peaks for iron at 6.404 and 7.058 keV, confirming the presence of Fe_3O_4 in the fibers. Heparinized fibers also exhibited a sulfur characteristic peak at 2.308 keV.

Further analysis of heparin on the fibers was performed using LC-MS. The fibers were first incubated in a buffer solution containing the enzymes heparinase I, II and III overnight. The resulting disaccharide mixture was then chromatographically separated and the eluate was evaluated by MS and compared to a mixture of heparin disaccharide standards. Both cellulose-Fe_3O_4-heparin core−shell nanofibers and mixed nanofibers showed all disaccharide peaks corresponding to disaccharide peaks present in the heparin starting material. Since EDX reveals mostly surface composition, this helped confirm that heparin was enzymatically accessible on the surface of the nanofibers (see Supporting Information).

Cotton (raw material), cellulose, and the composite nanofibers were subjected to thermogravimetric analysis (TGA) to study the thermal behavior of the fibers (see Figure 7). The fibers were heated from room temperature to 600 °C at 20 °C/min in dry air. The cotton raw material showed greater thermal stability by decomposing at a higher temperature compared to electrospun cellulose nanofibers. The decomposition temperatures of cotton and cellulose nanofibers were ca. 350 and 320 °C, respectively. In contrast, the composite nanofibers all decomposed at lower temperatures. Monofilament fibers demonstrated the lowest decomposition temperatures from ca. 300 to 320 °C. Pure sodium heparin shows decomposition at ca. 250 °C and leaves a residual mass of 39.5%, which is consistent with the ash content observed for heparin.[41] Monofilament fibers exhibited rapid degradation and retained the highest residual mass (17.2%). This rapid degradation at lower temperatures is likely due in part to the highly heterogeneous nature of the monofilament fibers. Cellulose−Fe_3O_4 core−shell fibers and cellulose−-Fe_3O_4 core−shell nanofibers with immobilized heparin leave a residual mass of 7.0% and 11.8%, respectively. This increase in residual mass percentage is consistent with the corresponding presence of magnetite and heparin in the composite fibers. The presence of iron in the core of core−shell fibers was also quantified by TGA. The monofilament cellulose fibers, cellulose−Fe_3O_4 fibers, and cellulose−Fe_3O_4 heparinized fibers were each examined by TGA. The pure cellulose nanofibers decomposed from 250 to 350 °C and left <5% residual mass. The cellulose−Fe_3O_4 core−shell fibers showed a similar decomposition range but left ca. 15% residual mass. The cellulose-Fe_3O_4 core−shell fibers with immobilized heparin on shell decomposed from 250 to 330 °C and left ca. 15% residual mass. This study shows that core−shell fibers allow for higher inclusion of Fe_3O_4 NPs in the fibers during electrospinning. The TGA data fails to detect a peak corresponding to the flash point of room temperature ionic liquid (164 °C), which suggests that no residual RTIL exists in the fiber samples. Complete removal of RTIL can be ensured by running fibers through a Soxhlet extractor with hot water for 24 h, but this was not deemed necessary in the current work as no evidence for residual RTIL was observed.

The XRD pattern of the Fe_3O_4 NPs used to prepare the composite fibers showed face-centered cubic crystal structure (crystallographic space group $Fd\bar{3}m$) and matched well with the lattice parameters (i.e., $a = b = c = 8.398$ and $\alpha = \beta = \gamma = 90°$). All the patterns show the two characteristic peaks of cellulose (see Figure 8).[25] The presence of these Fe_3O_4 NPs in the composite fibers was confirmed by the appearance of characteristic peaks at $2\theta = 30.088$, 35.439, 43.070, 56.958, and 62.546° corresponding to crystal planes (220), (311), (400), (511), and (440), respectively.[41] According to the XRD patterns obtained, it is clear that the crystal structure of the Fe_3O_4 NPs has been retained in the composite fibers. In contrast to core−shell fibers containing Fe_3O_4, the intensity of the XRD peaks of the monofilament fibers was substantially

DOI: 10.1021/acsbiomaterials.6b00273
ACS Biomater. Sci. Eng. 2016, 2, 1905−1913

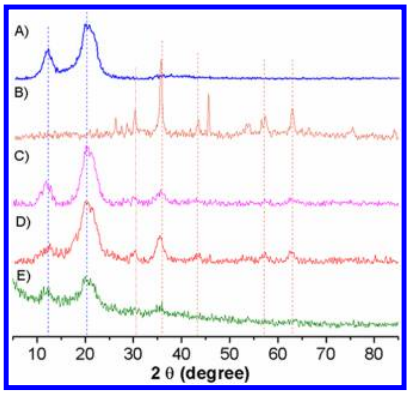

Figure 8. XRD sprectra of Fe_3O_4 NPs and nanofiber composites. A) cellulose nanofibers, B) Fe_3O_4 NPs, C) cellulose-Fe_3O_4 core-shell fiberswith immobilized heparin on shell, D) cellulose-Fe_3O_4-heparin monofilament fibers, E) cellulose-Fe_3O_4 core-shell fibers with heparin blended into the shell.

larger, likely due to the presence of Fe_3O_4 NPs on the surface of the fibers.

The anticoagulant activity of the heparin on composite fibers was investigated using two amydolytic assays (see Table S1). Chromogenic antifactor IIa and antifactor Xa assays test the antithrombin III-mediated activity of heparin. These assays measure the inhibition of the activity of factor Xa and thrombin (factor IIa) in the presence of the serine protease inhibitor antithrombin III. These serine proteases are two important factors in the blood coagulation cascade. First, heparin binds to antithrombin III to form binary complex. This complex then inactivates the factor IIa or factor Xa reducing their activity and the amount of *p*-nitrophenol chromogen (405 nm), produced through the service protease catalyzed hydrolysis specific chromogenic peptide substrates. Therefore, the amount of heparin present is inversely proportional to the absorbance at 405 nm. Electrospun nanofiber samples were assayed and the results were compared with a blank and a positive control. Cellulose-Fe_3O_4-heparin monofilament fibers and both the cellulose-Fe_3O_4 core−shell nanofibers with heparin either blended into or immobilized onto the shell layer showed a significant decrease in absorbance at 405 nm, confirming the presence of accessible bioactive heparin on the composite fiber surface.

This novel nanofibrous polymer material has a potential of being used in a broad range of biomedical applications such as in biocompatible valves in the body that could be opened and closed magnetically. The initial applications could in vitro where magnetically addressable, blood-compatible fibers with conjugated antibodies could be added to blood (ex vivo in an extracorporeal circuit) without the requirement of anti-coagulation to bind specific proteins or toxins removal of from the blood. These fibers could also be used to prepare nonwoven membranes for blood filtration circuits that could be moved into the blood flow for filtration and out of the blood flow for cleaning/defouling. In vivo applications are much further in the future but may take the form of a magnetically actuated nonwoven heart valve that can be seeded with cells and implanted. Alternatively they could be used in the purification of heparin binding proteins or in blood collection and ex vivo blood diagnostics. An interesting direction for future research would be the use of heparin to selectively bind proteins in blood with membranes modified with heparin to obtain the retention of desired proteins. Considering that membranes are heavily used in the downstream separations train of biologics, heparin-modified membranes would be interesting to investigate.

CONCLUSION

Magnetically responsive heparin-immobilized cellulose nanofiber composites were successfully synthesized by a wet-wet electrospinning from the RTIL [EMIM][Ac]. Fe_3O_4 NPs were successfully incorporated into the fibers homogeneously in monofilament fibers or heterogeneously in the core−shell fiber composition. This magnetic NP impregnation of the fibers enabled the manipulation of nonwoven fiber membranes in both dry and wet states by an external magnetic field. Three distinct types of nanocomposite fibers were developed, which sought to address possible biocompatibility and long-term stability issues. TGA, LC-MS, FTIR and XRD provided detailed compositional analysis for these nanocomposite fibers, confirming the presence of each component and the surface accessibility of the heparin. The anticoagulant activity of immobilized heparin on the nanocomposite fiber surfaces was confirmed by antifactor Xa and antifactor IIa assays.

ASSOCIATED CONTENT

Supporting Information

The Supporting Information is available free of charge on the ACS Publications website at DOI: 10.1021/acsbiomaterials.6b00273.

Details on the LC-MS, heparin composition, TEM, FTIR, and EDX (PDF)

Video S1, mixed fibers movie (M4V)

Video S2, magnetite cellulose core shell fibers with covently bound heparin (M4V)

AUTHOR INFORMATION

Corresponding Author

*E-mail: simmot@rpi.edu. Tel: (518) 276-3849.

Author Contributions

The study was performed by L.H., W.M.R.N.U., and A.P., and the manuscript was written by W.D., Y.Z., R.J.L., and T.J.S. All authors have given their approval to the final version of this manuscript.

Author Contributions

†L.H. and W.M.R.N.U. contributed equally.

Notes

The authors declare no competing financial interest.

ACKNOWLEDGMENTS

The authors acknowledge the helpful guidance of the manager of the electron microscopy laboratory, Mr. Raymond P. Dove III Esq., for SEM and TEM assistance, and the analytical core facility director, Dr. Joel Morgan, for XRD and TGA assistance. We also thank Dr. Xing Zhang for assistance in activation of cellulose fibers, Dr. Aki Onishi for assistance in running the antifactor Xa and antifactor IIa assays, and Dr. Lei Lin for conducting the LC-MS analysis.

REFERENCES

(1) Zheng, Y.; Monty, J.; Linhardt, R. J. Polysaccharide-based nanocomposites and their applications. *Carbohydr. Res.* **2015**, *405*, 23−32.

DOI: 10.1021/acsbiomaterials.6b00273
ACS Biomater. Sci. Eng. 2016, 2, 1905−1913

(2) Javid, A.; Ahmadian, S.; Saboury, A. A.; Kalantar, S. M.; Rezaei-Zarchi, S. Novel biodegradable heparin-coated nanocomposite system for targeted drug delivery. *RSC Adv.* **2014**, *4*, 13719−13728.
(3) Li, J.; Hou, Y.; Chen, X.; Ding, X.; Liu, Y.; Shen, X.; Cai, K. Recyclable heparin and chitosan conjugated magnetic nanocomposites for selective removal of low-density lipoprotein from plasma. *J. Mater. Sci.: Mater. Med.* **2014**, *25*, 1055−1064.
(4) Lee, J. H.; Jung, M. J.; Hwang, Y. H.; Lee, Y. J.; Lee, S.; Lee, D. Y.; Shin, H. Heparin-coated superparamagnetic iron oxide for in vivo MR imaging of human MSCs. *Biomaterials* **2012**, *33*, 4861−4871.
(5) Kemp, M. M.; Linhardt, R. J. Heparin-based nanoparticles. *WIREs Nanomed. Nanobiotechnol.* **2010**, *2*, 77−87.
(6) Kemp, M. M.; Kumar, A.; Mousa, S.; Dyskin, E.; Yalcin, M.; Ajayan, P.; Linhardt, R. J.; Mousa, S. A. Gold and silver nanoparticles conjugated with heparin derivative possess anti-angiogenesis properties. *Nanotechnology* **2009**, *20*, 455104−11.
(7) Park, T.-J.; Lee, S.-H.; Simmons, T. J.; Martin, J. G.; Mousa, S. A.; Snezhkova, E. A.; Sarnatskaya, V. G.; Nikolaev; Linhardt, R. J. Heparin−cellulose−charcoal composites for drug detoxification prepared using room temperature ionic liquids. *Chem. Commun.* **2008**, 5022−5024.
(8) Wu, B.; Gerlitz, B.; Grinnell, B. W.; Meyerhoff, M. E. Polymeric coatings that mimic the endothelium: Combining nitric oxide release with surface-bound active thrombomodulin and heparin. *Biomaterials* **2007**, *28*, 4047−4055.
(9) Linhardt, R.; Murugesan, S.; Xie, J. Immobilization of heparin-approaches and applications. *Curr. Top. Med. Chem.* **2008**, *8*, 80−100.
(10) Zheng, Y.; Miao, J.; Zhang, F.; Cai, C.; Koh, A.; Simmons, T. J.; Mousa, S. A.; Linhardt, R. J. Surface modification of a polyethylene film for anticoagulant and anti-microbial catheter. *React. Funct. Polym.* **2016**, *100*, 142−150.
(11) Capila, I.; Linhardt, R. J. Heparin-Protein Interactions. *Angew. Chem., Int. Ed.* **2002**, *41*, 390−412.
(12) Yang, H. S.; La, W. G.; Bhang, S. H.; Jeon, J. Y.; Lee, J. H.; Kim, B. S. Heparin-conjugated fibrin as an injectable system for sustained delivery of bone morphogenetic protein-2. *Tissue Eng., Part A* **2010**, *16*, 1225−1233.
(13) Singh, S.; Wu, B. M.; Dunn, J. C. Y. The enhancement of VEGF-mediated angiogenesis by polycaprolactone scaffolds with surface cross-linked heparin. *Biomaterials* **2011**, *32* (8), 2059−2069.
(14) Knaack, S.; Lode, A.; Hoyer, B.; Rosen-Wolff, A.; Gabrielyan, A.; Roeder, I.; Gelinsky, M. Heparin modification of a biomimetic bone matrix for controlled release of VEGF. *J. Biomed. Mater. Res., Part A* **2014**, *102* (10), 3500−3511.
(15) She, Z.; Liu, W.; Feng, Q. Silk fibroin/chitosan/heparin scaffold: preparation, antithrombogenicity and culture with hepatocytes. *Polym. Int.* **2010**, *59* (1), 55−61.
(16) Lu, A.-H.; Salabas, E. L.; Schuth, F. Magnetic nanoparticles: Synthesis, protection, functionalization and application. *Angew. Chem., Int. Ed.* **2007**, *46*, 1222−1244.
(17) Miyauchi, M.; Simmons, T. J.; Miao, J.; Gagner, J. E.; Shriver, Z. H.; Aich, U.; Dordick, J. S.; Linhardt, R. J. Electrospun polyvinylpyrrolidone fibers with high concentrations of ferromagnetic and superparamagnetic nanoparticles. *ACS Appl. Mater. Interfaces* **2011**, *3*, 1958−1964.
(18) Sheikh, L.; Mahto, N.; Nayar, S. In situ synthesis of hydroxyapatite nanocomposites using iron oxide nanofluids at ambient conditions. *J. Mater. Sci.: Mater. Med.* **2015**, *26*, 47−55.
(19) Park, T.-J.; Murugesan, S.; Linhardt, R. J. *Polysaccharide Materials: Performance by Design*; ACS Symposium Series; American Chemical Society: Washington, D.C., 2009; Vol. *1017*, pp 133−149.
(20) Miyamoto, T.; Takahashi, S.; Ito, H.; Inagaki, H.; Noishiki, Y. Tissue biocompatibility of cellulose and its derivatives. *J. Biomed. Mater. Res.* **1989**, *23*, 125−133.
(21) Dugan, J. M.; Gough, J. E.; Eichhorn, S. J. Bacterial cellulose scaffolds and cellulose nanowhiskers for tissue engineering. *Nanomedicine* **2013**, *8* (2), 287−298.
(22) Miyauchi, M.; Miao, J.; Simmons, T. J.; Dordick, J. S.; Linhardt, R. J. Flexible electrospun cellulose fibers as an affinity packing material for the separation of bovine serum albumin. *J. Chromatogr. Sep. Tech.* **2011**, *2* (2), 110.
(23) Zheng, Y.; Cai, C.; Zhang, F.; Monty, J.; Linhardt, R. J.; Simmons, T. J. Can natural fibers be a silver bullet? Antibacterial cellulose fibers through the covalent bonding of silver nanoparticles to electrospun fibers. *Nanotechnology* **2016**, *27*, 055102.
(24) Teo, W. E.; Ramakrishna, S. A review on electrospinning design and nanofiber assemblies. *Nanotechnology* **2006**, *17*, R89−R106.
(25) Zheng, Y.; Miao, J.; Maeda, N.; Frey, D.; Linhardt, R. J.; Simmons, T. J. Uniform Nanoparticle Coating Of Cellulose Fibers During Wet Electrospinning. *J. Mater. Chem. A* **2014**, *2*, 15029−15034.
(26) Miyauchi, M.; Miao, J.; Simmons, T. J.; Lee, J.-W.; Doherty, T. V.; Dordick, J. S.; Linhardt, R. J. Conductive cable Fibers with insulating surface prepared by coaxial electrospinning of multi-walled nanotubes and cellulose. *Biomacromolecules* **2010**, *11*, 2440−2445.
(27) Fuller, J.; Carlin, R. T.; De Long, H. C.; Haworth, D. Structure of 1-ethyl-3-methylimidazolium hexafluorophosphate: Model for room temperature molten salts. *J. Chem. Soc., Chem. Commun.* **1994**, *3*, 299−300.
(28) Meli, L.; Miao, J.; Dordick, J. S.; Linhardt, R. J. Electrospinning from room temperature ionic liquids for biopolymer fiber formation. *Green Chem.* **2010**, *12*, 1883−1892.
(29) Huddleston, J. G.; Visser, A. E.; Reichert, W. M.; Willauer, H. D.; Broker, G. A.; Rogers, R. D. Characterization and comparison of hydrophilic and hydrophobic room temperature ionic liquids incorporating the imidazolium cation. *Green Chem.* **2001**, *3*, 156−164.
(30) Carda-Broch, S.; Berthod, A.; Armstrong, D. W. Solvent properties of the 1-butyl-3-methylimidazolium hexafluorophosphate ionic liquid. *Anal. Bioanal. Chem.* **2003**, *375*, 191−199.
(31) Meli, L.; Miao, J.; Dordick, J. S.; Linhardt, R. J. Electrospinning from room temperature ionic liquids for biopolymer fiber formation. *Green Chem.* **2010**, *12*, 1883−1892.
(32) Farran, A.; Cai, C.; Sandoval, M.; Xu, Y.; Liu, J.; Hernaiz, M. J.; Linhardt, R. J. Green solvents in carbohydrate chemistry: From raw materials to fine chemicals. *Chem. Rev.* **2015**, *115*, 6811−6853.
(33) Simmons, T. J.; Lee, S. H.; Miao, J.; Miyauchi, M.; Park, T.-J.; Bale, S. S.; Pangule, R.; Bult, J.; Martin, J. G.; Dordick, J. S.; Linhardt, R. J. Preparation of synthetic wood composites using ionic liquids. *Wood Sci. Technol.* **2011**, *45*, 719−733.
(34) Viswanathan, G.; Murugesan, S.; Pushparaj, V.; Nalamasu, O.; Ajayan, P. M.; Linhardt, R. J. Preparation of biopolymer fibers by electrospinning from room temperature ionic liquids. *Biomacromolecules* **2006**, *7*, 415−418.
(35) Tsuruta, T.; Hayashi, T.; Kataoka, K.; Ishihara, K.; Kimura, Y. (Eds.), *Biomedical Applications of Polymeric Materials*; CRC Press: Boca Raton, FL, 1993.
(36) Lohse, D. L.; Linhardt, R. J. Purification and characterization of heparin lyases from Flavobacterium heparinum. *J. Biol. Chem.* **1992**, *267* (34), 24347−24355.
(37) Yafuso, M.; Linhardt, R. J. Process to activate sulfated polysaccharides. 1996, U.S. Patent 5583213.
(38) Leslie, D. C.; Waterhouse, A.; Berthet, J. B.; Valentin, T. M.; Watters, A. L.; Jain, A.; Kim, P.; Hatton, B. D.; Nedder, A.; Donovan, K.; Super, E. H.; Howell, C.; Johnson, C. P.; Vu, T. L.; Bolgen, D. E.; Rifai, S.; Hansen, A. R.; Aizenberg, M.; Super, M.; Aizenberg, J.; Ingber, D. E. A bioinspired omniphobic surface coating on medical devices prevents thrombosis and biofouling. *Nat. Biotechnol.* **2014**, *32* (11), 1134−1140.
(39) Axen, R.; Porath, J.; Ernback, S. Chemical coupling of peptides and proteins to polysaccharides by means of cyanogen halides. *Nature* **1967**, *214*, 1302−1304.
(40) Scott, D. A.; Charles, A. F. Studies on Heparin: III. The Purification of Heparin. *J. Biol. Chem.* **1933**, *102*, 437−448.
(41) Small, A. C.; Johnston, J. H. Novel hybrid materials of magnetic nanoparticles and cellulose fibers. *J. Colloid Interface Sci.* **2009**, *331*, 122−126.

DOI: 10.1021/acsbiomaterials.6b00273
ACS Biomater. Sci. Eng. 2016, 2, 1905−1913